3

Manipulating Nematic Liquid Crystals-based Magnetophotonic Crystals

Hai-Xia Da and Z.Y. Li
Department of Physics and Jiangsu Key Laboratory of Thin films, Soochow University, Suzhou, 215006, China

1. Introduction

Magnetic materials have attracted considerable attention for their applications in high density magneto-optical storage devices, which is not only appealing scientifically, but also makes the magnetic materials promising for a wide range of applications [1-11]. Due to their unique optical properties, magnetic materials have been introduced into the photonic crystals, forming magnetophotonic crystals (MPCs), i.e., the photonic crystals with at least one magnetic material component [2,3]. Now the optical properties can be mediated and controlled by the external electric or magnetic field due to the existence of magnetic materials. The special importance of MPCs can be ascribed to the existence of magneto-optical effects, for example, Kerr effect and Faraday rotation [12-28]. They were discovered by Kerr and Faraday, respectively, and are now widely used in integrated optics and magneto-optical devices for magnetic domain imaging, mapping of hysteresis loops and high density recording [6].

Magnetic materials with large magneto-optical responses are always the attractive ones used in magnetophotonic crystals. In contrast to the corresponding three-dimensional magnetic structures, magnetic materials exhibit a larger magneto-optical effects due to the light's confinement in the MPCs, offering a genuine chance to put their optical responses into applications. The optimized MPCs have been shown to behave like mixed systems, with a coexistence of high transmittance and large magneto-optical effects [12-28]. All possible configurations are proposed to achieve strong magneto-opitcal effects, including the ordinary cavity-based, multilayered periodic and aperiodic structures. Furthermore, the diffracted magneto-optical enhancement is also demonstrated in the grating structures theoretically and experimentally, which greatly reduces the thickness of the device contrary to multilayered structures and miniaturizes magneto-optical devices in integrated optics [29,30].

The ability to tune the otpical properties by an external stimulus is a key issue of modern optoelectronics. Although most attention has so far been focused on the magneto-optical properties of the given structures, tunable magneto-optical devices have important applications and will be respected in optical switches and displays. There are few reports concerning with the tunable magnetophotonic crystals [31-33]. For example, it is possible to manipulate the magnetic order of magnetic conducting spheres using the magnetic field, thus forming the tunable magnetophotonic crystals [31]. Semiconductor quantum well has

Source: New Developments in Liquid Crystals, Book edited by: Georgiy V. Tkachenko,
ISBN 978-953-307-015-5, pp. 234, November 2009, I-Tech, Vienna, Austria

been discussed as possible candidates for achieving artificial tunable MPCs [32]. From the application-oriented perspective it would be very desirable if tunable magneto-optical effects could be achieved by controlling applied electric fields, thus making such effect a potential proposition. Therefore, to search the alternate scheme is of great importance in tunable magneto-optical electronics. It was known that nematics liquid crystals (NLCs) are good choices for tunable photonic crystals due to their unique sensitivity to temperature, the electric, magnetic field, or lights itself [34]. However, seldom reports concerning tunable magneto-optical effects based on the NLCs have been presented in the literatures. Therefore, it would be interesting to investigate a possible way of creating electrically controlled magneto-optical effects in the MPCs with the NLCs. The application of liquid crystals in the MPCs offers new opportunities for the tunable optoelectronic devices.

Liquid crystals are materials that display a phase of matter whose properties lie between those of a conventional liquid and a solid crystal. They are a class of materials particularly attractive for liquid crystal displays and optical electronic applications due to their high sensitivity to the external stimulus and have been studied experimentally extensively [35-37]. There are three basis kinds of liquid crystals: NLCs, cholesteric liquid crystals and smectic liquid crystals [38-47]. Here we only focus attention on the NLCs, which is characterized by molecules that have no positional order but tend to align along the same direction. Due to thermal random motion, friction and collision between molecules, not all molecules align along a certain direction and their directions vary around the average direction randomly. This average direction is referred to as the orientation of the liquid crystal, which stands for the average direction of most molecules. This parameter, i.e., the director, is an important factor to denote the liquid crystal's properties. Normally, the light waves with electric fields perpendicular or parallel to the director of a NLC have ordinary n_o or extraordinary n_e refractive indices, respectively. Therefore, the refractive index of a NLC may be changed between n_o and n_e by controlling the orientation of the directors using the applied electric field or adjusting the temperature [34]. Specifically, the refractive index of NLC is especially easy to control using the external electric field in one-dimensional cases [38-40]. Previous studies have demonstrated, experimentally as well as theoretically, how tunability is brought to electro-optical systems by employing NLCs, such as the realization of tunable band gaps in one-, two-, and three-dimensional photonic crystals based on NLCs [34, 38-40]. Tunable negative refraction is also achieved at the interface between air and the NLC, and that the refraction can be adjusted by an applied electric field or by the temperature [48-50]. Multistable all-optical switching have been demonstrated by utilizing an unique nonlinear coupling between light and the NLC in a periodic dielectric structure [51]. The absorption peak of nanoparticles doped in the NLC can be controlled by the external electric field [52]. The light-induced reorientational effects have been observed in a one-dimensional photonic crystal with the NLCs [53]. Especially, the orientation of the magntic anisotropy from ferromagnetic nanorods have been manipulated by means of electric fields in the composite of liquid crystals and ferromagnetic nanorods [54]. While the investigations of the magnetic properties in a electrically controlled way is still in infancy, the current experimental work suggests a possible chance of realizing the tunable MPCs with liquid crystals for fundamental research and practical applications.

Moreover, the particular nonreciprocity of magnetic materials, i.e., the polarized state (right/left handed polarized light) will switch into the opposite one (left/right handed polarized light) when the direction of the incident light is reversed, makes the MPCs

remarkable workbenches for the unidirectional electromagnetic transmission [55-61]. Such a character shown in the cavity-based, periodic and aperiodic multilayered structures has made them good candidates to be isolators, unidirectional transmitted MPCs and one way waveguides with MPCs [57-59]. It has been unraveled that both ternary and microcavity configurations combined with waveguides can generate the isolators and circulators [55]. The asymmetric isolators are shown to be much efficient compared with symmetric ones [62]. The performance of small antennas embedded within MPCs constructed from periodic arrangements of homogenous and anisotropic material layers was demonstrated that the extraordinary high gain and enhanced power reception can be achieved [63]. Furthermore, it has been demonstrated that the optical Tamm states (OTS) can be observed in one dimensional MPCs in recent theoretical and experimental works [64-70]. There will be considerable interest to exploit and identify the OTS in the MPCs. The ability of creating and manipulating the surface states is central to the development of subwavelength microscopy. However, few reports concerning the tunable OTS in MPCs have been presented [66]. Therefore, it is interesting to find whether the NLCs can be used to realize the OTS in MPCs, or more importantly, whether such a configuration will support the controllable OTS. Controlling the OTS by electrical means is particularly interesting, as that would allow the integration of magnetic materials and the NLC with conventional optical electronics. Due to these unique optical properties, the MPCs with the NLC will hold substantial promise for possible optoelectronic devices.

In this chapter, we present a theoretical investigation on the NLC-based MPCs by performing a 4×4 transfer matrix method [71-73]. The optical properties of the MPCs with the NLCs will be reminiscent of both components. The coupling between the incident waves and the magnetic materials creates the magneto-optical effects, while the component of the NLCs is now responsible for its tunability occurring in the present configurations. The chapter is organized as follows: In Sec. II, we give a general description of the 4×4 transfer matrix method, which is a consequence of the combination of Maxwell equations and constitutive relations. The relations between the reflected, transmitted field vectors and the incident field vectors are listed to elucidate the magnitude of magneto-optical effects. In Section III, the case of periodic structure is considered, i.e., one dimensional MPC whose unit cell is composed of alternating NLCs and magnetic materials. In this part, the NLC is treated as a simple isotropic dielectric material approximately [74]. In Sec. IV, one-dimensional MPC infiltrated with the NLC is investigated, where the intrinsic anisotropic properties of the NLC are taken into account. Combined with transfer matrix method and a piecewise homogeneity approximation method for the NLC [75], the magneto-optical effects of MPCs with the NLC is definitely achieved. In Sec. V, the tunable OTS is reported theoretically in the MPCs with the NLC. Finally, we give a summary about this work.

Our investigations reveal a variety of interesting results which are the main characteristics of one-dimensional MPCs with the NLC. The magneto-optical effects appear the peaks due to the abnormal dispersion relations at the edge of the band gaps. It is shown the shift of the peaks and the enhanced values in the magneto-optical spectrum as the permittivity of NLCs increases, which demonstrates that the magneto-optical effects can be altered by changing the permittivity in the NLCs. When the NLC-based cavity structure is subject to the applied electric field, the magneto-optical effects are observed to exhibit the similar trends as those of the periodic one treating the NLC as an approximate isotropic dielectric material. A significant shift of the peaks in the magneto-optical spectrum is observed with the external

voltage due to the directors' reorientation. In addition, the existence of intra-Brillouin-zone band gaps is demonstrated and they are predicted to be dependent on the applied voltages in the MPC with the NLC. If the present MPC is attached to the other photonic crystals with two dielectric materials, the OTS is also observed in the transmission spectrum and can be controlled by the applied voltages. Our results provide an approach to modify a interface state in a controllable manner, which is significant to its potential applications. Moreover, it is possible to design a larger tunable magneto-optical effects by simply selecting the appropriate liquid crystals in the MPCs with the NLC. The ability of creating the electrically-controlled magneto-optical effects can provide an extra space to be explored in the future. Such tunability of the magneto-optical effect may be useful for future application in electro-optical devices.

2. Theoretical treatment

A 4×4 transfer matrix method is an effective way to explore the optical properties of one dimensional multilayered configurations, which has been proved to be accurate enough to tackle the band structures of the uniaxial, bi-axially anisotropic dielectric materials and liquid crystals [71-72]. For the sake of convenience, we describe the theoretical method and detailed treatment in this section.

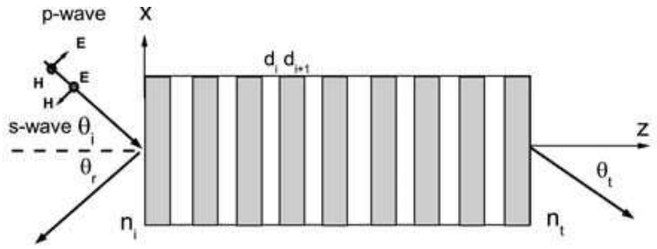

Fig. 1. Schematic view of the multilayered structure.

Fig. 1 shows a typical multilayered structure, which is sandwiched to the incident medium with the refractive index n_i and transmitted medium with the refractive index n_t, respectively. The incident wave vector is expressed as $\vec{k_i} = k_0(v_x, v_y, v_z)$, where $k_0 = \omega/c$, ω is the angular frequency of the incident wave, and c stands for the velocity of light in the vacuum. Here an electromagnetic wave impinges on the multilayered structure with an angle θ_i, which is confined in the x –z plane indicating $k_y = 0$, $v_x = n_i \sin\theta$ and $v_z = n_i \cos\theta$. The dielectric permittivity and magnetic permeability of any component are characterized by the tensors:

$$\vec{\vec{\varepsilon}} = \begin{pmatrix} \varepsilon_{11} & \varepsilon_{12} & \varepsilon_{13} \\ \varepsilon_{21} & \varepsilon_{22} & \varepsilon_{23} \\ \varepsilon_{31} & \varepsilon_{32} & \varepsilon_{33} \end{pmatrix}, \qquad \vec{\vec{\mu}} = \begin{pmatrix} \mu_{11} & \mu_{12} & \mu_{13} \\ \mu_{21} & \mu_{22} & \mu_{23} \\ \mu_{31} & \mu_{32} & \mu_{33} \end{pmatrix}. \tag{1}$$

For a monochrome light propagating along the z - axis with a given frequency ω, based on Maxwell's equations, we have [71]

$$\frac{d\Psi(z)}{dz} = \frac{i\omega}{c}\Delta(z)\Psi(z), \tag{2}$$

where $\Psi(z)$ is the field vector provided as $\Psi(z) = (E_x, H_y, E_y, -H_x)^t$, and $\Delta(z)$ is the Berrmeman matrix which is the function of the permittivity, permeability of the material and the incident wave vector. The subscript t denotes the transpose operator. The components of the Berreman matrix are provided with [71]

$$\begin{aligned}
t_{11} &= -v_{\mathrm{x}}\tfrac{\varepsilon_{31}}{\varepsilon_{33}} \\
t_{12} &= -\tfrac{v_{\mathrm{x}}^2}{\varepsilon_{33}} + \mu_{22} - \tfrac{\mu_{23}\mu_{32}}{\mu_{33}} \\
t_{13} &= -v_{\mathrm{x}}\tfrac{\varepsilon_{32}}{\varepsilon_{33}} + v_{\mathrm{x}}\tfrac{\mu_{23}}{\mu_{33}} \\
t_{14} &= -\mu_{21} + \tfrac{\mu_{23}\mu_{31}}{\mu_{33}} \\
t_{21} &= \varepsilon_{11} - \tfrac{\varepsilon_{13}\varepsilon_{31}}{\varepsilon_{33}} \\
t_{22} &= -v_{\mathrm{x}}\tfrac{\varepsilon_{13}}{\varepsilon_{33}} \\
t_{23} &= \varepsilon_{12} - \tfrac{\varepsilon_{13}\varepsilon_{32}}{\varepsilon_{33}} \\
t_{24} &= 0 \\
t_{31} &= 0 \\
t_{32} &= -\mu_{12} + \tfrac{\mu_{13}\mu_{32}}{\mu_{33}} \\
t_{33} &= -v_{\mathrm{x}}\tfrac{\mu_{13}}{\mu_{33}} \\
t_{34} &= \mu_{11} - \tfrac{\mu_{13}\mu_{31}}{\mu_{33}} \\
t_{41} &= \varepsilon_{21} - \tfrac{\varepsilon_{23}\varepsilon_{31}}{\varepsilon_{33}} \\
t_{42} &= -v_{\mathrm{x}}\tfrac{\varepsilon_{23}}{\varepsilon_{33}} + v_{\mathrm{x}}\tfrac{\mu_{32}}{\mu_{33}} \\
t_{43} &= \varepsilon_{22} - \tfrac{\varepsilon_{23}\varepsilon_{32}}{\varepsilon_{33}} - \tfrac{v_{\mathrm{x}}^2}{\mu_{33}} \\
t_{44} &= -v_{\mathrm{x}}\tfrac{\mu_{31}}{\mu_{33}}
\end{aligned} \tag{3}$$

Eq. (2) has a solution of the form:

$$\Psi(z) = \Psi(z_0)e^{i\frac{\omega}{c}\Delta(z-z_0)}, \tag{4}$$

Within the frame of transfer matrix method, the field vector can be expressed as,

$$\Psi(z) = T(z, z_0)\Psi(z_0). \tag{5}$$

where $T(z, z_0)$ is the transfer matrix provided with the Cauchy and Hamilton theorem [71]:

$$T(z, z_0) = \beta_0 I + \beta_1\Delta + \beta_2\Delta^2 + \beta_3\Delta^3, \tag{6}$$

These coefficients β_i are:

$$\begin{aligned}
\beta_0 &= -\sum_{i=1}^{4} \lambda_j\lambda_k\lambda_l \frac{f_i}{\lambda_{ij}\lambda_{ik}\lambda_{il}}, \\
\beta_1 &= \sum_{i=1}^{4} (\lambda_j\lambda_k + \lambda_j\lambda_l + \lambda_k\lambda_l) \frac{f_i}{\lambda_{ij}\lambda_{ik}\lambda_{il}}, \\
\beta_2 &= -\sum_{i=1}^{4} (\lambda_j + \lambda_k + \lambda_l) \frac{f_i}{\lambda_{ij}\lambda_{ik}\lambda_{il}}, \\
\beta_3 &= \sum_{i=1}^{4} \frac{f_i}{\lambda_{ij}\lambda_{ik}\lambda_{il}}.
\end{aligned} \tag{7}$$

where

$$\begin{aligned}
&\lambda_{ij} = \lambda_i - \lambda_j, \\
&f_i = e^{i\frac{\omega}{c}\lambda_i(z-z_0)}, \\
&i, j, k, l = 1, 2, 3, 4.
\end{aligned} \tag{8}$$

λ_i are the eigenvalues of the Berreman matrix. In contrast with the isotropic materials, it is more complicate due to the existence of the non-diagonal elements in the dielectric permittivity or magnetic permeability tensors. Even the incident plane wave is a linear polarization, it will form the non-linear polarized waves. Therefore, it typically yields the four solutions for the anisotropic materials, two of which represent left- and right- handed polarized forward propagating waves and another two are the corresponding backward propagating waves. If the individual layer occupies the spatial region of $z_0 < z < z_0+d$, the field vectors $\Psi(z_0 + d)$ and $\Psi(z_0)$ can be connected with

$$\Psi(z_0 + d) = T_i\Psi(z_0). \tag{9}$$

where T_i is the single-layer transfer matrix and d is the thickness of this layer. For the finite photonic crystals, the total transfer matrix T_{total} of the system can be achieved by multiplying the individual transfer matrix together. The NLC is of spatially inhomogeneity, whose treatment needs to adapt the piecewise homogeneity approximation method [75].
(E_i^p, E_i^s), (E_r^p, E_r^s) and $(E_t^p, E_t^s)$are used to describe the electric field components of the incident, reflected and transmitted waves, respectively. Subscript $p(s)$ denotes electromagnetic wave parallel (perpendicular) to the incident plane x –z, respectively. The incident, reflected and transmitted field vectors are expressed as

$$\begin{aligned}
\Psi_i &= \left(E_i^p \cos\theta_i, n_i E_i^p, E_i^s, n_i E_i^s \cos\theta_i\right)^t; \\
\Psi_r &= \left(-E_r^p \cos\theta_i, n_i E_r^p, E_r^s, -n_i E_r^s \cos\theta_i\right)^t; \\
\Psi_t &= \left(E_t^p \cos\theta_t, n_t E_t^p, E_t^s, n_t E_t^s \cos\theta_t\right)^t.
\end{aligned} \tag{10}$$

Due to the continuous boundary conditions of electronic and magnetic fields, the equation $\Psi_t = T(\Psi_i + \Psi_r)$ should be satisfied. Accordingly, the relations between the reflected, transmitted and incident waves are connected with [79]

$$\begin{pmatrix} E_r^p \\ E_r^s \end{pmatrix} = R \begin{pmatrix} E_i^p \\ E_i^s \end{pmatrix} = \begin{pmatrix} r_{pp} & r_{ps} \\ r_{sp} & r_{ss} \end{pmatrix} \begin{pmatrix} E_i^p \\ E_i^s \end{pmatrix}, \tag{11}$$

$$\begin{pmatrix} E_t^p \\ E_t^s \end{pmatrix} = T \begin{pmatrix} E_i^p \\ E_i^s \end{pmatrix} = \begin{pmatrix} t_{pp} & t_{ps} \\ t_{sp} & t_{ss} \end{pmatrix} \begin{pmatrix} E_i^p \\ E_i^s \end{pmatrix}, \tag{12}$$

where R (T) is the Jones reflectance (transmitted) matrices and r_{ij} (t_{ij}) is the ratio of the incident j polarized electric field and the reflected (transmitted) i polarized electric field. Then, the magneto-optical effects, i.e., Kerr effect and Faraday effect can be determined by [79]

$$\Theta_K^p = \theta_p + i\eta_p = \frac{r_{ps}}{r_{pp}}, \tag{13}$$

$$\Theta_K^s = \theta_s + i\eta_s = \frac{r_{sp}}{r_{ss}}. \tag{14}$$

$$\Theta_F^p = \theta_p + i\eta_p = \frac{t_{ps}}{t_{pp}}, \tag{15}$$

$$\Theta_F^s = \theta_s + i\eta_s = \frac{t_{sp}}{t_{ss}}. \tag{16}$$

where $\theta_{K,F}^p$ ($\theta_{K,F}^s$) and $\eta_{K,F}^p$ ($\eta_{K,F}^s$) are the Kerr/Faraday rotation angle and the ellipticity for the p(s) polarized wave, respectively. Based on these equations, the magneto-optical effects and the corresponding transmission/reflectance coefficients can be obtained directly.

3. Electrically-controlled magneto-optical effects in magnetophotonic crystals consisting of magnetic materials and NLC

In this part, we investigate the magneto-optical effects of a one dimensional MPC whose unit cell is composed of a magnetic material and NLC and give a detailed explanation to the obtained results.

Generally, the permittivity of NLC is provided by $\varepsilon_{LC} = \frac{\varepsilon_o \varepsilon_e}{\varepsilon_o \cos^2\theta + \varepsilon_e \sin^2\theta}$ for linear polarized light incident as an extraordinary wave onto it, where ε_o and ε_e are the respective dielectric permittivities for light polarized parallel and perpendicular to the director axis $\hat{n}$ [74]. It is noted that the only factor which affects the value of the permittivity of NLC is the director axis orientation angle θ with respect to the optical wave vector. Normally, losses are negligible for typical micron thick NLC in the optical frequency region. In the following numerical simulation, we treat the NLC as a homogeneous isotropic dielectric layer with the permittivity of ε_{LC} approximately, which simplify the calculations greatly [74]. In our model, we apply an electric field to control the director axis orientation θ of the aligned NLC with respect to the wave vector, which results in the variation of the extraordinary refractive

index from $n_\perp\ (\theta = 0°)$ to $n_\parallel\ (\theta = \frac{\pi}{2})$. The corresponding range of dielectric permittivity of NLC, ε_{LC}, is taken as 2 ≤ ε_{LC} ≤ 3 from nematic liquid crystal $5CB\ (\Delta n_{LC} \simeq 0.18)$ [34].

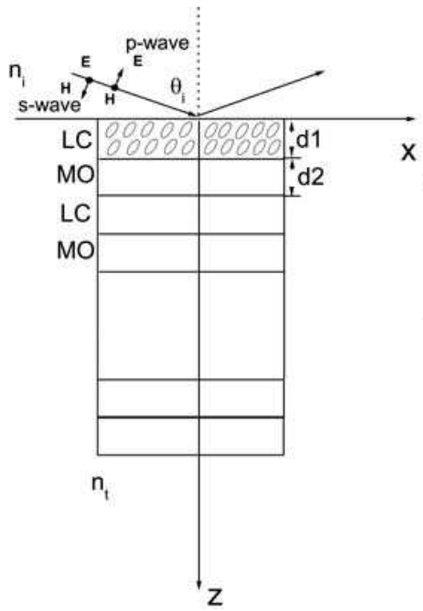

Fig. 2. One dimensional MPC consisting of the NLC and magnetic materials.

Fig. 2 shows a schematic illustration of a one-dimensional finite MPC, i.e., (NLC/magnetic materials). In the calculations, the total periodic number N is taken as 8 and the thicknesses of NLC and magnetic layers are d_1 = 500nm and d_2 = 20nm, respectively. The input and output media are supposed to be vacuum and glass, i.e., n_i = 1 and n_t = 1.5, respectively. The dielectric tensor of magnetic layers has an antisymmetric form and is denoted as [80]

$$\tilde{\varepsilon} = \begin{pmatrix} \varepsilon_{xx} & \cos\Theta\varepsilon_{xy} & -\sin\Theta\sin\Phi\varepsilon_{xy} \\ -\cos\Theta\varepsilon_{xy} & \varepsilon_{yy} & \sin\Theta\cos\Phi\varepsilon_{xy} \\ \sin\Theta\sin\Phi\varepsilon_{xy} & -\sin\Theta\cos\Phi\varepsilon_{xy} & \varepsilon_{zz} \end{pmatrix}. \tag{17}$$

where the magnetization vector makes an angle Θ with the z axis and its projection on the x –y plane makes the azimuth Φ with the x axis. As an illustrative example, the permittivity parameters of magnetic material are taken as ε_{xx} = ε_{yy} = ε_{zz} = –4.8984 + 19.415 i, ε_{xy} = $-\varepsilon_{yx}$ = 0.4322 + 0.0058i [81] while the permeability of magnetic material is nearly 1 at the optical frequency. Note that there are three cases according to the different values of Θ and Φ: the polar Kerr effect (Θ = Φ = 0), the longitudinal Kerr effect (Θ=$\frac{\pi}{2}$,Φ = 0) and the transverse Kerr effect (Θ, Φ = $\frac{\pi}{2}$). Here we only focus attention on the polar Kerr effect since the other two cases can be treated in the same way. The Kerr rotation angles as a function of the incident wavelength for different ε_{LC} are calculated when the light is incident normally to MPC. Since normal incident light leads to decoupling between p- and s-polarized waves and the two polarized lights are degenerate, only results for the p-wave are presented in the following figures.

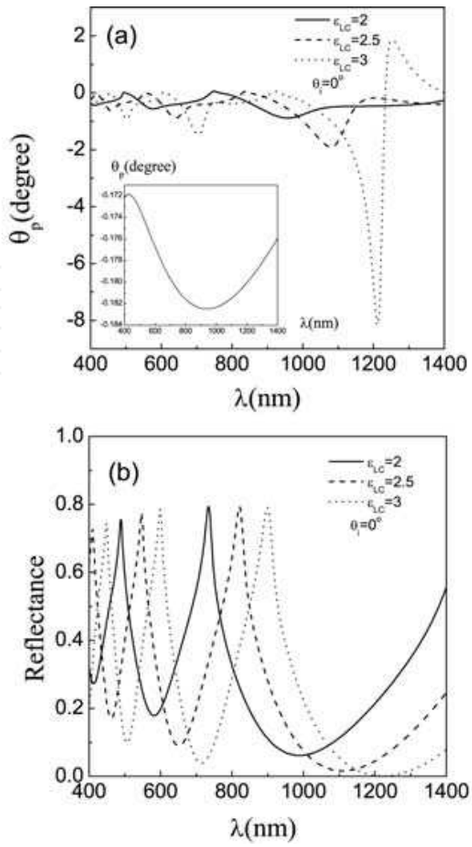

Fig. 3. (a) θ_p versus the incident wavelength under the dielectric permittivities of LCs ε_{LC} = 2, 2.5, 3 at the normal incident angle, are shown by solid, dash and dotted lines, respectively. (b) The dependence of the reflectance on the wavelength with the same conditions as Fig. 3(a). The inset in (a) shows θ_p in a single magnetic material with the thickness d = 20nm.

The solid, dash and dotted lines in Fig. 3 (a) describe the behaviors of θ_p for ε_{LC} = 2, 2.5, 3, respectively. Though the choice of the value of ε_{LC} seems arbitrary, the general tendency can still be seen clearly in the figures. Compared with the wavelength dependence of θ_p of a single magnetic layer as shown in the inset of Fig. 3(a), the Kerr rotation angles exhibited in the NLC-based MPC structures are enhanced dramatically, especially at certain wavelengths. The maximum value of θ_p increases from θ_{pmax} = –0.86° for ε_{LC} = 2 up to –8° for ε_{LC} = 3. The latter is nearly 40 times larger than that of the single magnetic layer(θ_{pmax} = –0.19°). The enhancement of θ_p compared with the single magnetic layer originates from the weak localization of light caused by the multiple interference due to the nonreciprocal properties of the Kerr effect [2]. Furthermore, the emergence of the θ_p-peaks is also an important feature of the multilayered structure in our MPC model. It is well-known that the Kerr effect is strengthened dramatically due to the abnormal dispersion relation at the edges of the photonic band gaps [28]. To make it more clear, Fig. 3 (b) shows the dependence of the reflectance of MPC on the wavelength. We clearly observe that the positions of the remarkable enhancement of θ_p are coincident with the positions of photonic band gap exactly.

Note that all the peaks in Fig. 3(a) shift towards longer wavelengths when the NLC's permittivity increases, which is particularly interesting since it reflects the good tunability of the Kerr effect in our model. A similar shift is also observed for the photonic band gaps as shown in Fig. 3(b). This result is reasonable since the positions of photonic band gaps depend on the wave impedance ratio of two components [82, 83], while the latter changes with the NLC's permittivity in the present case. For a rough estimation, the central wavelength of the NLC-based MPC structure can be evaluated by $\lambda_c = 2(n_{LC}d_1+n_m d_2)$ approximately [84], where n_m is the complex refractive index of magnetic layers and invariable with temperature or applied field. So the increase of the refractive index of NLC will directly lead to the enhancement of the central wavelength of the MPC structure. Since the refractive index of liquid crystal may be tuned between the ordinary and extraordinary refractive indices by controlling the orientation of the molecules under the influence of the applied electric field, the upper (lower) limit of the red shift is determined by the extraordinary (ordinary) permittivity, i.e., $\varepsilon_{LC} = 3$ ($\varepsilon_{LC} = 2$). Therefore, the NLC with larger optical anisotropy may behave as a better candidate for realizing larger tunability.

Fig. 3(a) also shows the significant increase of peak height with the permittivity of NLC in the spectrums of the Kerr rotation angle, which can be explained according to the circular birefringence. Different refractive indices due to different localization conditions, i.e., the localization wavelengths for left- and right- circular polarized lights, leads to the rotation of the reflected light [2]. In photonic crystals, the effective parameters of the unit cell can be expressed by the effective homogeneous anisotropic medium method [85]. The effective permittivity of MPC consisting of magnetic materials and NLC is given by

$$\varepsilon_{eff} = \begin{pmatrix} f_a\varepsilon_{LC} + f_b\varepsilon_{xx} & f_b\varepsilon_{xy} & 0 \\ f_b\varepsilon_{yx} & f_a\varepsilon_{LC} + f_b\varepsilon_{yy} & 0 \\ 0 & 0 & (f_a\varepsilon_{LC}^{-1} + f_b\varepsilon_{zz}^{-1})^{-1} \end{pmatrix}. \quad (18)$$

where $f_a = \frac{d_1}{d_1+d_2}$ and $f_b = \frac{d_2}{d_1+d_2}$. Note that the diagonal components of the effective permittivity depend on the permittivity of NLC but the non-diagonal components do not. Therefore, with the increase of ε_{LC}, the difference between the dielectric permittivity of the left- and right- circular polarized lights is enlarged, which leads to a relatively larger Kerr rotation angle at a longer wavelength.

Generally, refractive indices of liquid crystal are fundamentally interesting and practically useful parameters in the calculation of optical properties. By changing the permittivity of the liquid crystals, the magneto-optical effects varied in a controlled fashion, indicating that the engineering of magneto-optical devices relies on the control of the applied electric field. Here we focus attention on the change of the orientation of the molecules under the influence of the applied electric field at a fixed temperature. Actually, besides the external electric field, temperature is also an important factor affecting the liquid crystal refractive indices, which offers an alternative approach to control the magneto-optical effects, i.e., a temperature tunable MPC.

4. Voltage-controlled magneto-optical effects in cavity- based magnetophotonic crystal with the NLC

We have predicted that the opportunity of creating electrically controlled Kerr effect in magnetic multilayered structures [76]. It was suggested that a one-dimensional MPC composed of alternating NLC and magnetic materials can create tunable Kerr effect by considering the properties of liquid crystals and thus provide for tunable MPCs. However, we just employed an approximate isotropic treatment of NLC to analyze magneto-optical effects, which is a rough theoretical evaluation. It is generally known that the directors of NLCs exhibit inhomogeneous distribution under the influence of the applied electrical field [40]. Therefore, a rigorous anisotropic treatment of NLCs is employed to consider the NLC director's spatially inhomogeneous property upon an applied external voltage, which is based on the Newton method and continuous elastic theories. Although we expect such the tunable magneto-optical effect to be seen with a variety of patterns containing NLCs, we investigated a multilayered structure infiltrated with NLC, as shown schematically in Fig. 4. The defect of the NLC ensures that the present structure is sensitive to the external electric field and therefore shows the tunability of magneto-optical effects for observations at normal incidence.

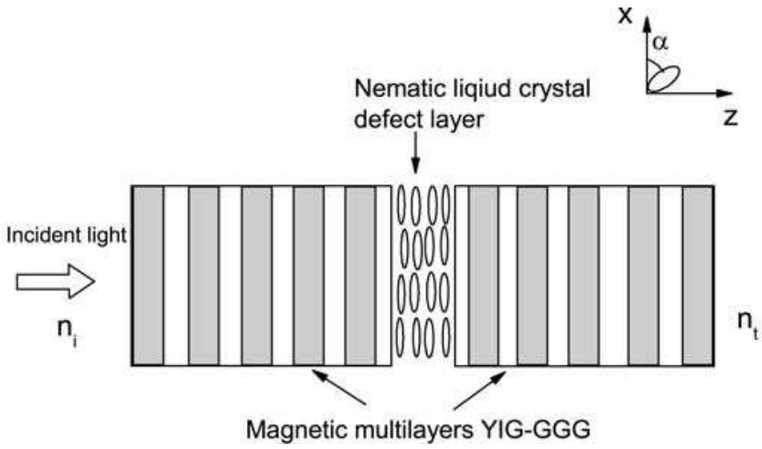

Fig. 4. The magnetophotonic crystal with the defect of NLC.

The gray and white regions are magnetic materials, yttrium-iron-garnet(YIG) and non-magnetic materials gadolinium-gallium garnet (GGG) with permittivity ε_2, respectively. The magnetization vector is oriented along the z axis in the YIG layers, which are characterized by antisymmetrical permittivity and have the following nonzero components, $\varepsilon_{xx} = \varepsilon_{yy} = \varepsilon_{zz} = \varepsilon_1$, $\varepsilon_{xy} = -\varepsilon_{yx} = ig$, where g is the gyrotropy of the magnetic layer. The thicknesses of magnetic and nonmagnetic materials are d_1 and d_2, respectively. The NLC is characterized by a long-range uniaxial orientational order of rod-like anisotropic molecules along a common director, whose dielectric tensor is given by [86]

$$\varepsilon_{LC} = \begin{pmatrix} n_0^2 + \Delta\varepsilon \cos^2\alpha & 0 & \Delta\varepsilon \cos\alpha \sin\alpha \\ 0 & n_0^2 & 0 \\ \Delta\varepsilon \cos\alpha \sin\alpha & 0 & n_0^2 + \Delta\varepsilon \sin^2\alpha \end{pmatrix}. \tag{19}$$

where α is the tilt angle between the principal axis of NLC molecule and the x axis. $\Delta\varepsilon$ is the optical dielectric anisotropy given as $n_e^2 - n_0^2$, n_0 and n_e are ordinary and extraordinary refractive indices, respectively. Upon an applied external voltage, the distribution of NLC director exhibits spatially inhomogeneous property. The distribution of α is given in the NLC slab by the Ossen Frank elastic theory when an electric field is applied along the z axis. The relations between α and the voltage V applied to NLC slab can be achieved in the light of the following equations [87]

$$(k_1 \cos^2\alpha + k_3 \sin^2\alpha)(\frac{dz}{d\alpha})^{-2} = \Delta\varepsilon_0 E^2(\sin^2\alpha_m - \sin^2\alpha), \tag{20}$$

$$\frac{V}{V_c} = \frac{2}{\pi}\int_0^{\pi/2}\sqrt{\frac{1+k\eta^2\sin^2\psi}{1-\eta^2\sin^2\psi}}d\psi, \tag{21}$$

with η = sin α_m and $k = (k_3 - k_1)/k_1$. The parameters k_1 and k_3 are the Frank elastic constants for splay and bend modes of the nematic director distortion, respectively. α_m is the maximum tilt angle in the NLC slab, $\Delta\varepsilon_0$ is the dielectric anisotropy at zero frequency. Note that the direction of NLC molecules is affected by the external voltage only when the applied voltage V exceeds a threshold value V_c $(= \pi\sqrt{k_1/\Delta\varepsilon_0})$.

For the one-dimensional multilayered structure $(GGG|YIG)^n(YIG|GGG)^m NLC(YIG|GGG)^n$, at the near infrared wavelength λ = 1.55μm, YIG and GGG are characterized by ε_1 = 5.5 + i0.0025, g = (1 – i0.15) ×10^{-2}, and ε_2 = 3.709, respectively [80]. The thicknesses are $d_1 = 0.466D$ and $d_2 = 0.534D$, respectively. k_1 = 7.4pN, k_3= 10.2pN, $\Delta\varepsilon_0$ = 1.43 ×10^{-10}F/m, n_e = 1.75, n_0 = 1.54 for typical NLC (5CB) [72], $d_{LC} = \frac{20}{6}D$. The repetition numbers are n = 16 and m = 29, respectively.

Fig. 5(a) corresponds to the distribution of α with different voltage V = 0, $2V_c$, $5V_c$ for p-polarized wave. The anisotropic character of NLC can be considered exactly by utilizing the obtained distribution of α. The calculated results for θ_p as functions of normalized frequency $\omega D/(2\pi c)$ with different voltages are plotted in Fig. 5(b). The solid, dashed, and dot-dashed lines correspond to θ_p with V = 0, $2V_c$, $5V_c$, respectively. It can be seen clearly that the spectrum of θ_p moves at different voltages, which is a direct manifestation of voltage-controlled Kerr effect. The frequency dependence of θ_p in the present case exhibits the following features. First, the positions of θ_p-peaks are dependent on the applied voltage due to the reorientation of the director. It is seen that the positions of peaks move toward high frequencies with the applied voltages. This is because of NLC's high sensitivity to the applied voltage. When the applied voltage is very small, the distribution of the director aligns x-direction due to the surface anchoring. With the increase of applied voltage, the energy of electric field adds gradually. When the applied voltage is bigger than the threshold value, the function of electric field plays a leading role. In such a case, the alignment of the director along the electric field can be observed. The reorientation of the NLC's director will lead to the change of its permittivity, which directly affects the Kerr rotation angles. Second, the amplitudes of θ_p depend strongly on the applied voltage, i.e., the

heights of θ_p-peaks increase considerably with the increase of V. For example, the maximum of θ_p at $V = 5V_c$ ($\theta_{p\,\max} = -30^\circ$) is approximately 3 times larger than that of θ_p ($\theta_{p\,\max} = -10^\circ$) at $V = 0$, which describes the large difference in the indices of refraction between the right and left circularly polarized light. This can be understood according to the circular birefringence, in which different refractive indices due to different localization wavelengths for left- and right- circularly polarized lights, leads to the large rotation of the reflected light [2]. In addition, the positions of θ_p-peaks agree with those of the dips in the reflection spectrum exactly. Take $V = 5V_c$ as an example, we calculated θ_p and the corresponding reflection spectrum, which are exhibited in Fig. 5(c) and (d). Such a phenomenon is directly related to the edges of photonic band gaps, where the abnormal dispersion relation leads to strong photonic localization. As a result, θ_p can be enhanced at these specific frequencies in the present structure [28].

Thus, the controllable magneto-optical effects have been predicted in the MPCs with the NLC, which will be a critical problem in the optoelectronic applications.

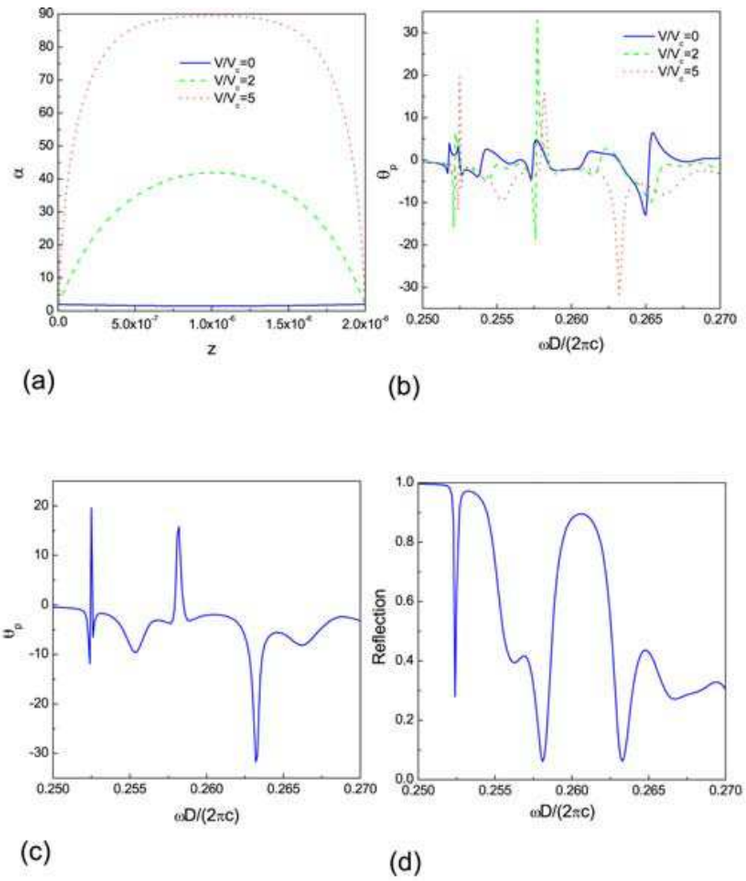

Fig. 5. (Color online) (a) α versus the distance at V =0,2Vc,5Vc, respectively; (b) θ_p versus the normalized frequency under V=0,2Vc,5Vc at the normal incident angle, are shown by solid, dashed, and dotted curves, respectively. (c) The dependence of θ_p and (d) the reflectance on the normalized frequency at V=5Vc.

5. Voltage-controlled tamm state in periodic magnetophotonic crystal with the NLC

The Tamm state proposed by Tamm is one of the most fundamental physical properties of the interface, which means electron states can occur in the energy band gap at a crystal surface [68]. In analogy with the electronic case, the OTS can be realized at the interface between two different photonic crystals with all isotropic dielectric materials. Conventional surface waves with a wave vector exceeding that of light in an incident medium decay exponentially away from the surface. In comparison with the conventional surface waves, the OTS can be formed for both the s– and p–polarized waves and occurs even at normal incidence [70]. In this part, we consider a one-dimensional MPC composed of the NLC and magnetic material, as illustrated in Fig. 6 (a). A linearly p-polarized monochromatic light impinges normally onto the structure. The thicknesses of the NLC and magnetic materials are d_1 and d_2, respectively. Due to the periodicity of the structure the eigenwaves satisfy Bloch's theorem, which leads to the equation det[P – e^{ikd}] = 0. Here P is the total propagation matrix of unit cell. Based on these equations, we may illustrate the characteristics of the normalized angular frequency and kd in the present configuration.

The parameters used in our calculations are taken as ε_1 = 3 and g = 0.5, where a larger value of g is used to make the band gaps easily observable. k_1 = 7.4pN, k_3= 10.2pN, $\Delta\varepsilon_0$ = 1.43 × 10^{-10} F/m, n_e = 1.75, n_0 = 1.54 for the NLC (5CB)[72], with the thicknesses d_1 = 0.5D, d_2 = 0.5D, respectively. The spatially inhomogeneous property of the directors is also taken into account in this calculation. In Fig. 7 (a), we present the $\omega d / c$ - kd characteristics under the applied voltages V = 0, $2V_c$, $5V_c$, respectively. From the figure it is clear that the intra-Brillouin-zone band gaps do occur and obviously depend on the applied voltages. This is a remarkable result in itself, as it indicates the existence and tunability of the OTS with the NLC. To understand qualitatively the origin of the appearance of intra-Brillouin-zone band gaps, we start with the simple case, i.e., we set the applied voltage as zero, where the distribution of the directors aligns along x-direction due to the surface anchoring. Now the NLC is a general anisotropic dielectric layer, where the eigenmodes are the ordinary and extraordinary waves when the incident wave enters into the NLC [88], then they become left- and right-circularly polarized waves in the magnetic materials. It appears an approximate standing wave due to the strong interference between these forward and backward waves, which leads to the formation of the intra-Brillouin-zone band gaps [65]. More interesting, the kd dependence on $\omega d/c$ in the present case exhibits the following feature, i.e., the intra-Brillouin-zone band gap moves with the applied voltages. The driving mechanism for manipulating the OTS arise from the intrinsic properties of the NLC. It is mainly caused by the sensitivity of the NLC on the applied voltage, which has significantly influence on the distribution of the NLC's directors. As widely known, the directors of the NLC molecules are affected by the external electric fleld only when the voltage V exceeds a threshold value V_c, where V_c is given by $V_c = \pi\sqrt{k_1/\Delta\varepsilon_0}$. The directors rotate parallel to the applied electric fleld to minimize the total free energy for V/V_c > 1. The reorientation of the NLC's directors leads to the variation of the effective refractive index, which change the optical path directly. Subsequently, the positions of standing waves will be finally changed with the applied voltages.

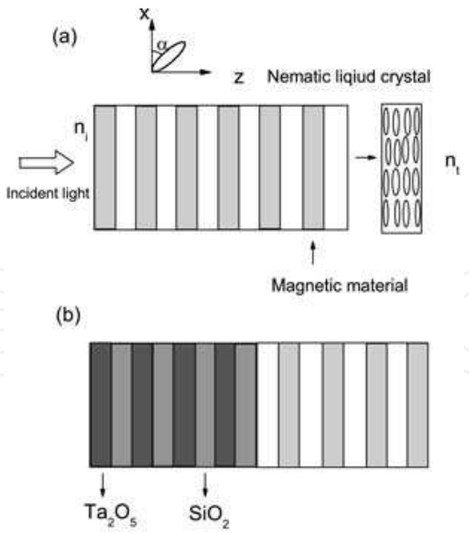

Fig. 6. (a) magnetophotonic crystal; (b) two adjoining photonic crystals, one of which consists of two dielectric materials and the other is composed of the NLC and magnetic material, i.e., $(Ta2O5 \mid SiO2)^8 (NLC \mid Bi : DyIG)^8$.

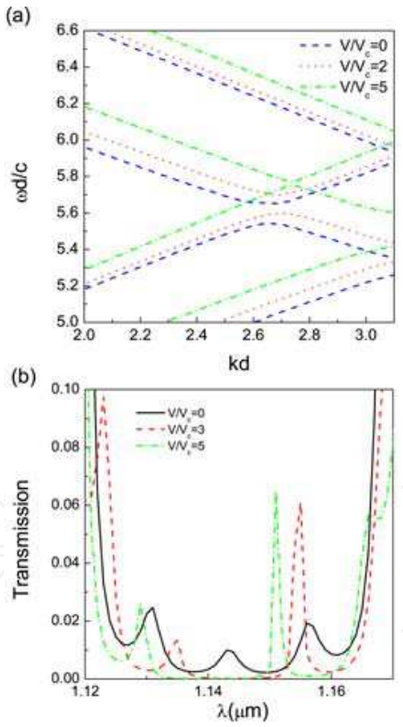

Fig. 7. (a) Normalized angular frequency $\omega * d/c$ versus kd at the normal incident angle under V = 0 (dash line), V = 2 Vc (dot line) and V = 5 Vc (dash dot line), respectively. ε_1 = 3 and g = 0.5 are used for the magnetic material. (b) The transmission of Fig. 6(b) versus λ at the normal incident angle under V = 0; 3 Vc; 5 Vc (solid, dash, and dash dot line), respectively. Here ε_{Ta2O5} = 4.41, ε_{SiO2} = 2.07, the realistic values ε_1 = 5.58 and g = –0.00198 are taken for Bi:DyIG.

Furthermore, two stacked photonic crystals are generally used to illuminate the existence of the OTS in experiments [64], which can be observed by studying the transmission/reflection spectra with a sharp narrow peak/dip in the finite photonic crystal. Thus, it is necessary for us to provide the transmission spectrum. We design the two stacked photonic crystals, shown in Fig. 6(b), one of which consists of two dielectric materials and the other is composed of the NLC and magnetic material. Now we use the realistic material parameters at the wavelength λ = 1.55μm, $\varepsilon_{Ta_2O_5}$ = 4.41, ε_{SiO_2} = 2.07, ε_1 = 5.58 and g = –0.00198 for Bi:DyIG. The thicknesses are $d_{Ta_2O_5}$ = 0.696μm, d_{SiO_2} = 1.37μm, d_{NLC} = 1μm and $d_{Bi:DyIG}$ = 1.77μm, respectively [67]. Fig. 7 (b) depicts the transmission of the two photonic crystals as a function of wavelength at normal incidence. It is observed that a sharp narrow peak indeed appears in the transmission spectrum. In particular, we notice two photonic crystals generate photonic gaps nearly from 1.12 – 1.17μm and 1.13 – 1.16μm, respectively. However, the peak appears in the band gaps of two photonic crystals, which significantly demonstrates the sharp peak comes from the resonant tunneling of the electromagnetic wave through the OTS at the interface. In addition, the peak undergoes slightly blueshift with the applied voltages, which manifest itself a good candidate to be a controlled OTS structure. Finally, it is noted that the existence of OTS survives for s-polarized wave but the tunability disappears because ε_{yy} is not dependent on the external voltage.

6. Conclusion

The tunable magneto-optical effects in magnetophotonic crystals with the NLC have been reviewed in this chapter. Two types of MPCs are studied, i.e., MPCs consisting of alternate magnetic materials and the NLC; the cavity-based MPCs with the NLC. Both of them exhibit the tunable magneto-optical properties qualitatively different from those of the unvariable MPCs without the NLC. It is predicted theoretically that the magneto-optical effects can be manipulated by the applied voltages in the theoretical treatments, i.e., the 4×4 transfer matrix method in combination with a piecewise homogeneity approximation for liquid crystals. A significant shift of the peaks' positions in magneto-optical spectrum is observed toward high frequencies with the applied voltages due to the high sensitivity of the directors on the external electric fields. By applying a tunable electric field, the voltage-induced reorientation of the directors of the NLCs alters the values of the dielectric permittivity in the NLC, thus leading to alternating magneto-optical effects. In addition, the tunable intra-Brillouin-zone band gaps can be realized in the MPCs with the NLC, which implies the existence of the OTS at the interface between two photonic crystals. The methods described here may possible to be implemented on many other periodic multilayered structures, cavity-based periodic structure, quasi-periodic and aperiodic structures, thus, opening the possibility to systematically investigate the magneto-optical effects in a controlled way. The structures we propose here is not only interesting in itself but also allows easy access to fabricate it in the experiments due to the mature techniques for one-dimensional systems. In fact, apart from the external applied electric field, the variation of temperature can also change the permittivity in the NLC component, and then alter the magneto-optical effects. It is obvious that there are a great space for the potential application of the MPCs with NLC. These results highlight an intriguing avenue for future

investigations in the development of tunable liquid crystal-based magnetophotonic crystals optoelectronic devices.

7. Acknowledgment

This project was supported by the National Natural Science Foundation of China under Grant No.10774107 and Jiangsu provincial innovation project under Grant No. ZY320607.

8. References

[1] M. Mansuripur, *The Principles of Magneto–Optical Recording* (Cambridge University Press, Cambridge, 1995).

[2] M Inoue, R Fujikawa, A Baryshev, A Khanikaev, P B Lim, H Uchida, O Aktsipetrov, A. Fedyanin, T Murzina and A. Granovsky, "Magnetophotonic crystals", J. Phys. D: Appl. Phys. 39, R151 (2006).

[3] Mitsuteru Inoue, Alexander V. Baryshev, Alexander B. Khanikaev Maxim E. Dokukin Kwanghyun Chung, Jinheo Hiroyuki Takagi, Hironaga Uchida, Pang Boey Lim, and Jooyoung Kim, "Magnetophotonic Materials and Their Applications", IEICE TRANS. ELECTRON, 91, 1630 (2008).

[4] R. Fujikawa, K. Tanizaki, A.V. Baryshev, P.B. Lim, K.H. Shin, H. Uchida, and M. Inoue, "Magnetic field sensors using magnetophotonic crystals", Proc. SPIE, 6369, 63690, (2006).

[5] J.H. Park, H. Takagi, K. Nishimura, et al., "Magneto-optic spatial light modulators driven by an electric field", J. Appl. Phys., 93, 8525, (2003).

[6] H.J. Park, J.K. Cho, K. Nishimura, and M. Inoue, "Magneto-optic spatial light modulator for volumetric digital recording system", Jpn. J. Appl. Phys., 41, 1813, (2002).

[7] Z.Wang and S. Fan, "Optical circulators in two-dimensional magneto-optical photonic crystals", Opt. Lett., 30, 1989, (2005).

[8] A.M. Merzlikin, A.P. Vinogradov, M. Inoue, et al., "The Faraday effect in two-dimensional magneto-photonic crystals", Journal of Magnetism and Magnetic Materials 300, 108, (2006).

[9] A.M. Merzlikin and A.P. Vinogradov, "Superprism effect in 1D photonic crystal", Opt. Commun. 259, 700, (2006).

[10] Belotelov VI, Kotov VA and Zvezdin AK, "New magnetooptical materials on a nanoscale", Phase Transitions, 79, 1135 (2006).

[11] Belotelov VI and Zvezdin AK, "Magneto-optical properties of photonic crystals", J. Opt. Soc. Am. B 22, 286 (2005).

[12] M. Inoue, K. Arai, T. Fujii and M. Abe, "Magneto-optical properties of one-dimensional photonic crystals composed of magnetic and dielectric layers", J. Appl. Phys. 83, 6768 (1998).

[13] M. Inoue and T. Fujii, "A theoretical analysis of magneto-optical Faraday effect of YIG films with random multilayer structures", J. Appl. Phys. 81, 5659, (1997).

[14] H. Kato and M. Inoue, "Reflection-mode operation of oned imensional magnetophotonic crystals for use in film-based magneto-optical isolator devices", J. Appl. Phys. 91, 7017, (2002).

[15] H. Kato, T. Matsushita, A. Takayama, et al., "Properties of one dimensional magnetophotonic crystals for use in optical isolator devices", IEEE Trans. Magn. 38, 3246, (2002).
[16] H. Kato, T. Matsushita, A. Takayama, M. Egawa, K. Nishimura, M. Inoue, "Theoretical analysis of optical and magneto-optical properties of one-dimensional magnetophotonic crystals", J. Appl. Phys. 93, 3906 (2003).
[17] Miguel Levy, "Normal modes and birefringent magnetophotonic crystals", J. Appl. Phys. 99, 073104 (2006).
[18] Miguel Levy, Rong Li, "Polarization rotation enhancement and scattering mechanisms in waveguide magnetophotonic crystals", Appl. Phys. Lett. 89, 121113 (2006).
[19] M. Levy and A.A. Jalali, "Band structure and Bloch states in birefringent one-dimensional magnetophotonic crystals: An analytical approach, J. Opt. Soc. Am. B 24, 1603, (2007).
[20] Khartsev SI and Grishin AM, "[Bi3Fe5O12/Gd3Ga5O12](m) magneto-optical photonic crystals", Appl. Phys. Lett. 87, 122504 (2005).
[21] S.I. Khartsev and A.M. Grishin, "High performance [Bi3Fe5O12/ Sm3Ga5O12]m magneto-optical photonic crystals", J. Appl. Phys. 101, 053906, (2007).
[22] A.B. Khanikaev, A.V. Baryshev, M. Inoue, et al., "Two-dimensional magnetophotonic crystal: Exactly solvable model", Phys. Rev. B 72, 035123, (2005).
[23] S. Sakaguchi and N. Sugimoto, "Multilayer films composed of periodic magneto-optical and dielectric layers for use as Faraday rotators", Opt. Commun. 162, 64 (1999).
[24] A.M. Merzlikin, A.P. Vinogradov, A.V. Dorofeenko, et al., "Controllable Tamm states in magnetophotonic crystal", Physica B 394, 277, (2007).
[25] A.P. Vinogradov, A.V. Dorofeenko, S.G. Erokhin, et al., "Surface state peculiarities in one-dimensional photonic crystal interfaces", Phys. Rev. B 74, 045128, (2006).
[26] I.L. Lyubchanskii, N.N. Dadoenkova, M.I. Lyubchanskii, et al., "Response of two-defect magnetic photonic crystals to oblique incidence of light: Effect of defect layer variation", J. Appl. Phys. 100, 096110, (2006).
[27] Kahl S, Grishin AM, "Enhanced Faraday rotation in all-garnet magneto-optical photonic crystal", Appl. Phys. Lett. 84, 1438 (2004).
[28] A. G. Zhdanov, A. A. Fedyanin, O. A. Aktsipetrov, D. Kobayashi, H. Uchida and M. Inoue, "Enhancement of Faraday rotation at photonic-band-gap edge in garnet-based magnetophotonic crystals", Journal of Magnetism and Magnetic Materials 300, 253 (2006).
[29] Yuehui Lu, Min Hyung Cho, JinBae Kim, YoungPak Lee, Jooyull Rhee, and Jae-Hwang Lee, "Control of Diffracted Magneto-Optical Enhancement in Ni Gratings", IEEE TRANSACTIONS ON MAGNETICS 44, 3300, (2008).
[30] Y. H. Lu, M. H. Cho, J. B. Kim,1 G. J. Lee, Y. P. Lee, and J. Y. Rhee, "Magneto-optical enhancement through gyrotropic gratings", Optics Express 16, 5378 (2008).
[31] M. Golosovsky, Y. Neve-Oz, and D. Davidov, "Magnetic-field-tunable photonic stop band in a three-dimensional array of conducting spheres", Phys. Rev. B 71, 195105 (2005).
[32] Jiang-Tao Liu and Kai Chang, "Tunable giant Faraday rotation of exciton in semiconductor quantum wells embedded in a microcavity", Appl. Phys. Lett. 90, 061114 (2007).

[33] S. V. Chernovtsev, D. P. Belozorov and S. I. Tarapov, "Magnetically controllable 1D magnetophotonic crystal in millimetre wavelength band", J. Phys. D: Appl. Phys. 40, 295C299 (2007).
[34] E. Graugnard, J. S. King, S. Jain, C. J. Summers, Y. Zhang-Williams, and I. C. Khoo, "Electricfield tuning of the Bragg peak in large-pore TiO2 inverse shell opals", Phys. Rev. B 72, 233105, (2005).
[35] P. Mach, P. Wiltzius, M. Megens, D. A. Weitz, K.-H. Lin, T. C. Lubensky, and A. G. Yodh, "Electro-optic response and switchable Bragg diffraction for liquid crystals in colloid-templated materials", Phys. Rev. E 65, 65, (2002).
[36] T. T. Larsen, A. Bjarklev, D. S. Hermann, and J. Broeng, "Optical devices based on liquid crystal photonic bandgap fibers", Optics Express 11, 2589, (2003).
[37] W. Hu, R. Dickie, R. Cahill, H. Gamble, Y. Ismail, V. Fusco, D. Linton, N. Grant, and S. Rea, "Liquid crystal tunable mm wave frequency selective surface", IEEE Microw. Wireless Compon. Lett. 17, 667, (2007).
[38] J. Cos, J. Ferre-Borrull, J. Pallares, L.F. Marsal, "Tunable FabryCProt filter based on one-dimensional photonic crystals with liquid crystal components", Optics Communications 282, 1220, (2009).
[39] V.G. Arkhipkin, V.A. Gunyakov, S.A. Myslivets, V.Ya. Zyryanov, and V.F. Shabanov, "Angular tuning of defect modes spectrum in the one-dimensional photonic crystal with liquid-crystal layer", Eur. Phys. J. E 24, 297 (2007).
[40] Ryotaro Ozakia and Hiroshi Moritake, Katsumi Yoshino, Masanori Ozaki, "Analysis of defect mode switching response in one-dimensional photonic crystal with a nematic liquid crystal defect layer", J. Appl. Phys. 101, 033503 (2007).
[41] Jiun-Yeu Chen and Lien-Wen Chen, "Polarization-dependent filters based on chiral photonic structures with defects", J. Opt. A: Pure Appl. Opt. 7 558, (2005).
[42] Hiroyuki Yoshida, Chee Heng Lee, Akihiko Fujii, and Masanori Ozaki, "Tunable Chiral Photonic Defect Modes in Locally Polymerized Cholesteric Liquid Crystals", Mol. Cryst. Liq. Cryst. 477, 255, (2007).
[43] Yuhua Huang, Ying Zhou, Charlie Doyle, and Shin-Tson Wu, "Tuning the photonic band gap in cholesteric liquid crystals by temperature-dependent dopant solubility", Optics Express, 14, 1236 (2006).
[44] N. Scaramuzza, C. Ferrero, B. V. Carbone, and C. Versace, "Dynamics of selective reflections of cholesteric liquid crystals subject to electric fields", J. Appl. Phys. 77, 572 (1995).
[45] Kuniaki Konishi, Benfeng Bai, Xiangfeng Meng, Petri Karvinen, Jari Turunen, Yuri. P. Svirko, and Makoto Kuwata-Gonokami, "Observation of extraordinary optical activity in planar chiral photonic crystals", Optics Express, 16, 7189 (2008).
[46] M V Gorkunov and M A Osipov, "Molecular theory of layer contraction in smectic liquid crystals, J. Phys. Condens. Mater 20, 465101 (2008).
[47] Barbero G and Komitov L, "Temperature-induced tilt transition in the nematic phase of liquid crystal possessing smectic C-nematic phase sequence", J. Appl. Phys. 105, 064516 (2009).
[48] Qian Zhao, Lei Kang, Bo Li, Ji Zhou, Hong Tang and Baizhe Zhang, "Tunable negative refraction in nematic liquid crystals", Appl. Phys. Lett. 89, 221918 (2006).

[49] Lei Kang, Qian Zhao, Bo Li, and Ji Zhoua, Hao Zhu, "Experimental verification of a tunable optical negative refraction in nematic liquid crystals", Appl. Phys. Lett. 90, 181931 (2007).

[50] Jeremy A. Bossard, Xiaotao Liang, Ling Li, Seokho Yun, Douglas H. Werner, E, Brian Weiner, Theresa S. Mayer, Paul F. Cristman, Andres Diaz, and I. C. Khoo, "Tunable Frequency Selective Surfaces and Negative-Zero-Positive Index Metamaterials Based on Liquid Crystals", IEEE Transactions on Antennas and Propagation, 56, 1308, (2008).

[51] Miroshnichenko AE, Brasselet E, Kivshar YS, "All-optical switching and multistability in photonic structures with liquid crystal defects", Appl. Phys. Lett. 92, 253306 (2008).

[52] Li-Hsuan Hsu, Kuang-Yao Lo, Shih-An Huang, Chi-Yen Huang, and Chung-Sung Yang, "Irreversible redshift of transmission spectrum of gold nanoparticles doped in liquid crystals", Appl. Phys. Lett. 92, 181112 (2008).

[53] Laudyn U A, Miroshnichenko A E, Krolikowski W, et al., "Observation of light-induced reorientational effects in periodic structures with planar nematic-liquid-crystal defects", Appl. Phys. Lett. 92, 203304 (2008).

[54] Lin TJ, Chen CC, Lee W, et al., "Electrical manipulation of magnetic anisotropy in the composite of liquid crystals and ferromagnetic nanorods", Appl. Phys. Lett. 93, 013108 (2008).

[55] Alexander B. Khanikaev and M. J. Steel, "Low-symmetry magnetic photonic crystals for non-reciprocal and unidirectional devices", Optics Express 17, 5265 (2009).

[56] Z. Wang, Y. D. Chong, J. D. Joannopoulos, and M. Soljacic, "Reflection-Free One-Way Edge Modes in a Gyromagnetic Photonic Crystal", Phys. Rev. Lett. 100, 01390501 (2008).

[57] Z. Yu, G. Veronis, Z. Wang, and S. Fan, "One-Way Electromagnetic Waveguide Formed at the Interface between a Plasmonic Metal under a Static Magnetic Field and a Photonic Crystal", Phys. Rev. Lett. 100, 02390201 (2008).

[58] Z. Yu, Z. Wang, and S. Fan, "One-way total reflection with one-dimensional magneto-optical photonic crystals", Appl. Phys. Lett. 90, 121133 (2007).

[59] A. Figotin and I. Vitebskiy, "Electromagnetic unidirectionality in magnetic photonic crystals", Phys. Rev. B 67, 165210 (2003).

[60] A. Figotin and I. Vitebskiy, "Nonreciprocal magnetic photonic crystals", Phys. Rev. E 63, 066609 (2001).

[61] K.-Y. Jung, B. Donderici, and F. L. Teixeira, "Transient analysis of spectrally asymmetric magnetic photonic crystals with ferromagnetic losses", Phys. Rev. B 74, 165207 (2006).

[62] Ruiyi Chen, Dongjie Tao, Haifeng Zhou, Yinlei Hao, Jianyi Yang, Minghua Wang and Xiaoqing Jiang, "Asymmetric multimode interference isolator based on nonreciprocal phase shift", Optics Communications 282 (2009) 862.

[63] Mumcu G., Sertel K., Volakis J.L., "Miniature Antennas and Arrays Embedded Within Magnetic Photonic Crystals", IEEE 5, 168 (2006).

[64] T. Goto, A.V. Dorofeenko, A. M. Merzlikin, A.V. Baryshev, A. P. Vinogradov, M. Inoue, A. A. Lisyansky, and A. B. Granovsky, "Optical Tamm States in One-Dimensional Magnetophotonic Structures", Phys. Rev. Lett. 101, 113902 (2008).

[65] Fei Wang, Akhlesh Lakhtakiab, "Intra-Brillouin-zone bandgaps due to periodic misalignment in one-dimensional magnetophotonic crystals", Appl. Phys. Lett. 92, 011115 (2008).
[66] A.M. Merzlikina, A.P. Vinogradova, A.V. Dorofeenkoa, M. Inoueb, M. Levyc, A.B. Granovskyd, "Controllable Tamm states in magnetophotonic crystal", Phys. B 394, 277 (2007).
[67] A. P. Vinogradov, A. V. Dorofeenko, S. G. Erokhin, M. Inoue, A. A. Lisyansky, A. M. Merzlikin, and A. B. Granovsky, "Surface state peculiarities in one-dimensional photonic crystal interfaces", Phys. Rev. B 74, 045128 (2006).
[68] I. E. Tamm, Phys. Z. Sowjetunion, "On the possible bound states of electrons on a crystal surface ", 1, 733 (1932).
[69] M. Kaliteevski, I. Iorsh, S. Brand, R. A. Abram, J. M. Chamberlain, A. V. Kavokin, and I. A. Shelykh, "Tamm plasmon-polaritons: Possible electromagnetic states at the interface of a metal and a dielectric Bragg mirror", Phys. Rev. B 76, 165415 (2007).
[70] A. V. Kavokin, I. A. Shelykh, and G. Malpuech1, "Lossless interface modes at the boundary between two periodic dielectric structures", Phys. Rev. B 72, 233102 (2005).
[71] H. Wohler, G. Haas, M. Fritsch, and D. A. Mlynski, "Faster 4 x 4 matrix method for uniaxial inhomogeneous media", J. Opt. Soc. Am. A 5, 1554 (1988).
[72] D. W. Berreman, "Optics in smoothly varying anisotropic planar structures: Application to liquid-crystal twist cells", J. Opt. Soc. Am. 63, 1374 (1973).
[73] H.X. Da, C. Xu, and Z.Y. Li, "Magneto-optical effect of left-handed material", Eur. Phys. J. B 45, 347 (2005).
[74] Yao-Yu Wang, and Lien-Wen Chen, "Tunable negative refraction photonic crystals achieved by liquid crystals ", Optics Express 14, 10580 (2006).
[75] A. Lakhtakia and R. Messier, "Sculptured Thin Films: Nanoengineered Morphology and Optics", SPIE Press, Bellingham, WA, USA, 2005.
[76] H. X. Da, P. Xu, J. C. Wu, and Z. Y. Li, "Electrically controlled Kerr effect in magnetophotonic crystals based on nematic liquid crystals", J. Appl. Phys. 104, 033911 (2008).
[77] Hai-xia Da, Zi-qiang Huang, and Z. Y. Li, "Voltage-controlled Kerr effect in magnetophotonic crystal", Opt. Lett. 34, 356 (2009).
[78] Hai-xia Da, Zi-qiang Huang, and Z. Y. Li, "Electrically-controlled Optical Tamm States in magnetophotonic crystal based on nematic liquid crystals", IN PRESS, OPTICS LETTERS.
[79] Chun-Yeol You and Sung-Chul Shin, "Novel method to determine the off-diagonal element of the dielectric tensor in a magnetic medium", Appl. Phys. Lett. 70, 2595 (1997).
[80] A. Zvezdin and V. Kotov, Modern Magneto–optics and Magneto–optical Materials (IOP, Bristol, 1997).
[81] K. Balasubramanian, A. Marathay, and H. A. Macleod, "Modeling Magneto-optical thin-film media for optical-data storage", Thin Solid Films 164, 391 (1988).
[82] C.-S. Kee, J. Y. Park, S. J. Kim, H. C. Song, Y. S. Kwon, N. H. Myung, S. Y. Shin, and H. Lim, "Essential parameter in the formation of photonic band gaps", Phys. Rev. E 59, 4695 (1999);

[83] C.-S. Kee, J.-E. Kim, H. Y. Park, and H. Lim, "Roles of wave impedance and refractive index in photonic crystals with magnetic and dielectric properties", IEEE Trans. Microwave Theory Tech. 47, 2148 (1999).
[84] A. Saib, D. Vanhoenacker-Janvier, I. Huynen Laboratoire, A. Encinas, L. Piraux, E. Ferain, and R. Legras, "Magnetic photonic band-gap material at microwave frequencies based on ferromagnetic nanowires", Appl. Phys. Lett. 83, 2378 (2003).
[85] R. H. Tarkanyan and D. G. Niarchos, "Effective negative refractive index in ferromagnet-semiconductor superlattices", Optics Express 14, 5433 (2006).
[86] I.-C. Khoo, *Liquid Crystals*, 1st ed (Wiley, New York, 1995), pp. 21-24.
[87] L. Liebert, *Liquid Crystals*, 1st ed (Academic, New York, 1978), pp. 81.
[88] P. Yeh, "Electromagnetic propagation in birefringent layered media", J. Opt. Soc. Am. 69, 742 (1979).

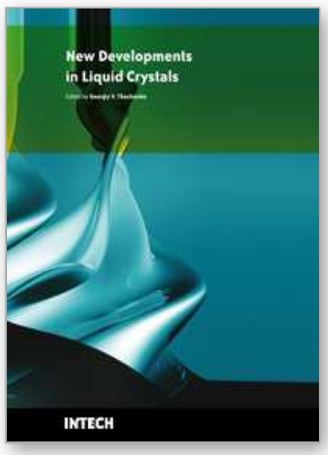

New Developments in Liquid Crystals

Edited by Georgiy V Tkachenko

ISBN 978-953-307-015-5
Hard cover, 234 pages
Publisher InTech
Published online 01, November, 2009
Published in print edition November, 2009

Liquid crystal technology is a subject of many advanced areas of science and engineering. It is commonly associated with liquid crystal displays applied in calculators, watches, mobile phones, digital cameras, monitors etc. But nowadays liquid crystals find more and more use in photonics, telecommunications, medicine and other fields. The goal of this book is to show the increasing importance of liquid crystals in industrial and scientific applications and inspire future research and engineering ideas in students, young researchers and practitioners.

How to reference

In order to correctly reference this scholarly work, feel free to copy and paste the following:

Hai-Xia Da and Z.Y. Li (2009). Manipulating Nematic Liquid Crystals-based Magnetophotonic Crystals, New Developments in Liquid Crystals, Georgiy V Tkachenko (Ed.), ISBN: 978-953-307-015-5, InTech, Available from: http://www.intechopen.com/books/new-developments-in-liquid-crystals/manipulating-nematic-liquid-crystals-based-magnetophotonic-crystals

INTECH
open science | open minds

InTech Europe
University Campus STeP Ri
Slavka Krautzeka 83/A
51000 Rijeka, Croatia
Phone: +385 (51) 770 447
Fax: +385 (51) 686 166
www.intechopen.com

InTech China
Unit 405, Office Block, Hotel Equatorial Shanghai
No.65, Yan An Road (West), Shanghai, 200040, China
中国上海市延安西路65号上海国际贵都大饭店办公楼405单元
Phone: +86-21-62489820
Fax: +86-21-62489821

IntechOpen